

Short communication

Characterization of LiMn_2O_4 -coated LiCoO_2 film electrode prepared by electrostatic spray deposition

Won-Sub Yoon^{a,*}, Kyung Yoon Chung^a, Kyung-Wan Nam^b, Kwang-Bum Kim^b

^a Chemistry Department, Brookhaven National Laboratory, Upton, New York 11973, USA

^b Division of Materials Science & Engineering, Yonsei University, 134 Shinchon-dong, Seodaemun-gu, Seoul 120-749, Korea

Received 8 August 2005; received in revised form 13 December 2005; accepted 20 December 2005

Available online 15 February 2006

Abstract

LiMn_2O_4 -coated LiCoO_2 film was synthesized by the ESD technique. The bulk structure and its electrochemical property were studied by X-ray diffraction (XRD) and cyclic voltammetry (CV) and the surface structure were characterized using soft XAS at the O K-edge and the Mn L-edge. The bulk structure and the electrochemical property of the LiMn_2O_4 -coated LiCoO_2 film do not show substantial difference compared to the bare LiCoO_2 film. The thermal stability of LiCoO_2 film is improved by LiMn_2O_4 coating on the surface of the LiCoO_2 film. The Mn L-edge and O K-edge results suggest that the structure at the surface of LiMn_2O_4 -coated LiCoO_2 film is a spinel $\text{LiCo}_x\text{Mn}_{2-x}\text{O}_4$.

© 2006 Elsevier B.V. All rights reserved.

Keywords: LiMn_2O_4 coating; Soft X-ray absorption spectroscopy; ESD; Lithium rechargeable batteries; Thin film

1. Introduction

LiCoO_2 is most widely used as the cathode material for both Li rechargeable batteries and thin-film microbatteries due to its advantages including high specific capacity, high operating voltage, and long cycle life [1–3]. LiCoO_2 thin films have been fabricated by several methods, such as r.f. magnetron sputtering, pulse laser deposition, and chemical vapor deposition. Recently, Schoonman et al. have developed the electrostatic spray deposition (ESD) method and applied it to fabricating thin-film cathode of rechargeable microbatteries [4,5]. The ESD technique offers many advantages over some conventional deposition techniques, such as a simple and low cost set-up, high deposition efficiency, low temperature synthesis, and easy control of the composition and surface morphology of the deposited films.

Recently, novel approaches that coat surface of cathode materials for Li batteries by various oxides have been conducted to improve electrode performance such as thermal stability, cyclability, high temperature capacity, and so on [6,7]. Similar approach has been also applied to the thin-film electrode for Li microbatteries [8]. These report clearly showed that the electrode performance is improved not by doping but by coat-

ing. Characterizations of the coated surface structure play an important role in understanding the improved electrochemical property by surface coating. Since these surface coatings on the cathode materials have nanoscale dimension, electronic and structural characterizations of the layer on the surface of the materials might not be easy.

Soft X-ray absorption spectroscopy (XAS) has been applied in the investigation of the electronic structure of electrode materials for Li rechargeable batteries [9–11]. Soft X-ray absorption spectra can be obtained in both the electron yield and fluorescence modes. The electron yield mode is surface sensitive (within ~ 50 Å) while the fluorescence yield mode is suitable for bulk studies (more than ~ 2000 Å) [12]. Therefore, soft XAS using electron yield mode can be an useful tool to characterize surface structure of those oxide-coated electrode materials. In this work, we prepared LiMn_2O_4 -coated LiCoO_2 films by the ESD technique. The bulk structure and its electrochemical property were studied by X-ray diffraction (XRD) and cyclic voltammetry (CV) and the surface structure were characterized using soft XAS at the O K-edge and the Mn L-edge.

2. Experimental

The ESD set-up used here and its working principles have been described in the literature [5,13]. A high dc voltage is

* Corresponding author. Tel.: +1 631 344 6145; fax: +1 631 344 5815.
E-mail address: wonsuby@bnl.gov (W.-S. Yoon).

applied between an electrically conductive substrate and a metal capillary nozzle, which is connected to a precursor solution. Under a suitable flow rate, the precursor solution is atomized at the orifice of the nozzle, generating a fine spray. The spray moves toward the heated substrate under the electrostatic force and, due to pyrolysis of the precursors, a thin layer is deposited on the substrate surface. An ethanol solution of $\text{LiNO}_3 + \text{Mn}(\text{NO}_3)_2$ with a molar ratio $\text{Li}:\text{Mn} = 1:2$ was used as the precursor solution (0.04 M). The precursor solution was pumped at a rate of 2 ml h^{-1} to a stainless steel nozzle, which placed 4 cm above LiCoO_2 film substrate. The total amount of Mn in the precursor solution corresponded to 3 mol% of LiCoO_2 film. The deposition temperature was chosen generally between 200 and 400°C . LiMn_2O_4 film on the LiCoO_2 substrate was annealed at 400°C . Electrochemical measurements were carried out using a three-electrode cell with 1 M LiClO_4 /propylene carbonate (PC) solution in a glove box. Li foils were used as the counter and reference electrodes.

The soft XAS measurements of the LiMn_2O_4 -coated LiCoO_2 films were performed on U7 beamline in the storage ring of 2.5 GeV with the ring current of 120–160 mA at Pohang Light Source (PLS) [14]. The U7 beamline, which consists of 4.3 m long, 7 cm period undulator and the variable-included angle plane-grating monochromator, provides the highly brilliant and monochromatic linear-polarized soft X-ray for the high resolution spectroscopy [15]. The O K-edge and Mn $L_{\text{II,III}}$ -edge XAS data were taken in a total electron yield mode, recording the sample current. The experimental spectra were normalized by reference signal from Au mesh with 90% transmission. The energy calibrations for O K-edge and Mn $L_{\text{II,III}}$ -edge were made using the L-edges data of pure V and Mn metal foils, respectively. According to the measured photon absorption spectra specified as the inner shell electron excitation for the Ar, N_2 and Ne gases, the energy resolving power ($E/\Delta E$) in entire measurement range was greater than 3000. The base pressure of the experiment chamber was in 10^{-8} mbar range.

3. Results and discussion

The LiMn_2O_4 was successfully coated on LiCoO_2 film electrode by electrostatic spray deposition technique. Fig. 1 shows XRD patterns for (a) LiCoO_2 and (b) LiMn_2O_4 -coated LiCoO_2 film on $\text{Pt}/\text{Al}_2\text{O}_3$ substrate. All diffraction peaks can be indexed by assuming the structure to be a hexagonal lattice of the α - NaFeO_2 type. There is no substantial difference between XRD patterns for LiCoO_2 and LiMn_2O_4 -coated LiCoO_2 film. This indicates that bulk structure of both samples is a well-developed layered HT- LiCoO_2 . Cyclic voltammogram (CV) for LiMn_2O_4 -coated LiCoO_2 film at a scan rate of 0.1 mV s^{-1} is shown in Fig. 2. Typical cyclic voltammogram of HT- LiCoO_2 is also observed, which is characterized by three sets of well-defined current peaks [16]. The cyclic voltammogram displays the main lithium intercalation and deintercalation peaks near 3.9 V. Two high voltage peaks observed above 4 V result from phase transition between ordered and disordered lithium ion arrangements in the CoO_2 framework.

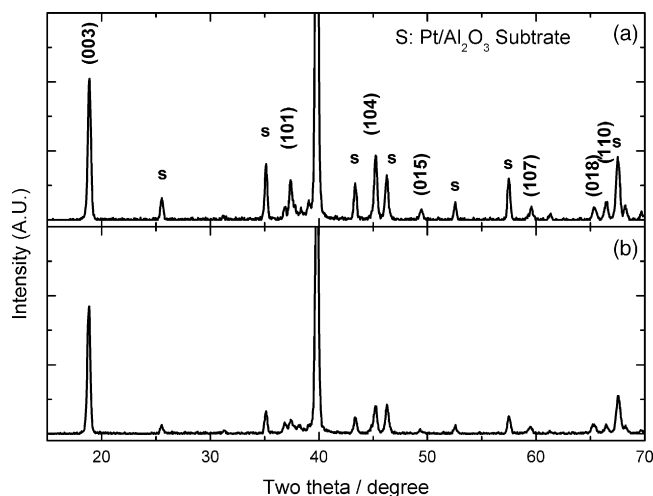


Fig. 1. XRD patterns for (a) LiCoO_2 and (b) LiMn_2O_4 -coated LiCoO_2 film on $\text{Pt}/\text{Al}_2\text{O}_3$ substrate.

Differential scanning calorimetry (DSC) test were carried out in order to investigate the thermal stability of the film electrodes. Unlike the XRD and CV results, DSC result of LiMn_2O_4 -coated LiCoO_2 film electrode is quite different from that of LiCoO_2 film electrode. Fig. 3 shows DSC scans of charged cathodes containing LiCoO_2 and LiMn_2O_4 -coated LiCoO_2 . For the pure LiCoO_2 cathode, the decomposition reaction appears to initiate at around 170°C , followed by development of intense exothermic peak in the temperature range of 180 – 200°C . This is consistent with the earlier report by Zhang et al. [17]. The overall heat generation under the exothermic peaks is a direct indication of the reactivity between the active materials and the electrolyte. The thermal behavior of the LiMn_2O_4 -coated LiCoO_2 is quite different from that for LiCoO_2 . The DSC scan of the LiMn_2O_4 -coated LiCoO_2 shows increase of the peak temperature and reduction of the exothermic peak compared to that of the LiCoO_2 , which indicates that LiMn_2O_4 -coated LiCoO_2 shows the good thermal stability of the cathode and reduction of the heat amount of the reaction.

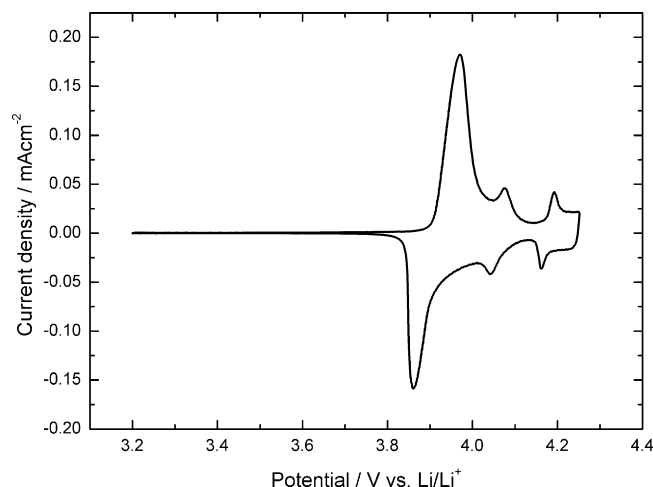


Fig. 2. Cyclic voltammograms for LiMn_2O_4 -coated LiCoO_2 film annealed at various temperature at a scan rate of 0.1 mV s^{-1} .

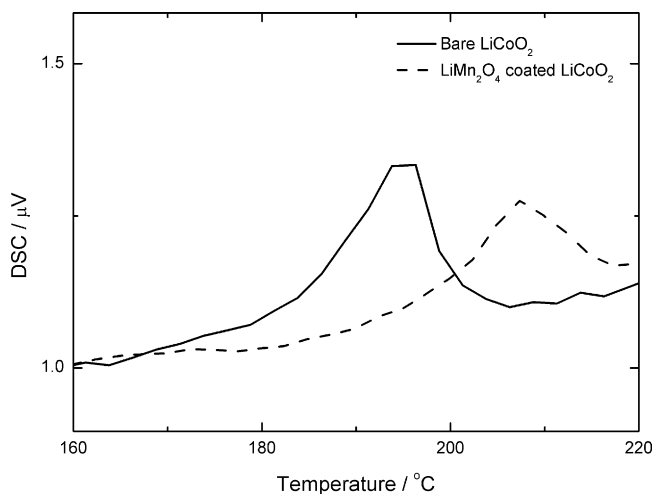


Fig. 3. DSC scans of charged cathodes containing bare and LiMn_2O_4 -coated LiCoO_2 . All the samples were equilibrated at 4.3 V before the DSC experiments.

Auger electron spectroscopy (AES) was carried out to examine the distribution of Mn atoms near the film surface. Fig. 4 shows concentration profiles of LiMn_2O_4 -coated LiCoO_2 film by the AES analysis. The concentration profiles clearly show that the Mn atoms are distributed only at the film surface region. It is reasonable that the relatively low firing temperature of 400°C limits diffusion of Mn ions inside the LiCoO_2 film resulting in the formation of a thin-film solid solution ($\text{LiCo}_x\text{Mn}_{2-x}\text{O}_4$) at the surface region.

Fig. 5 shows normalized Mn $L_{\text{II,III}}$ -edge X-ray absorption spectra of LiMn_2O_4 and LiMn_2O_4 -coated LiCoO_2 film using total electron yield mode that is surface sensitive (within $\sim 50 \text{ \AA}$). Because of the electric-dipole-allowed $2p \rightarrow 3d$ transition, the absorption peaks for the metal $L_{\text{II,III}}$ -edge XAS are relatively intense and are very sensitive to the oxidation state, spin state, and bond covalency. The electronic structure of the Mn ions in the surface of LiMn_2O_4 -coated LiCoO_2 film can be investigated qualitatively through peak features in the XAS spectra. There are two main peaks of L_{III} and L_{II} edges which are due to electronic

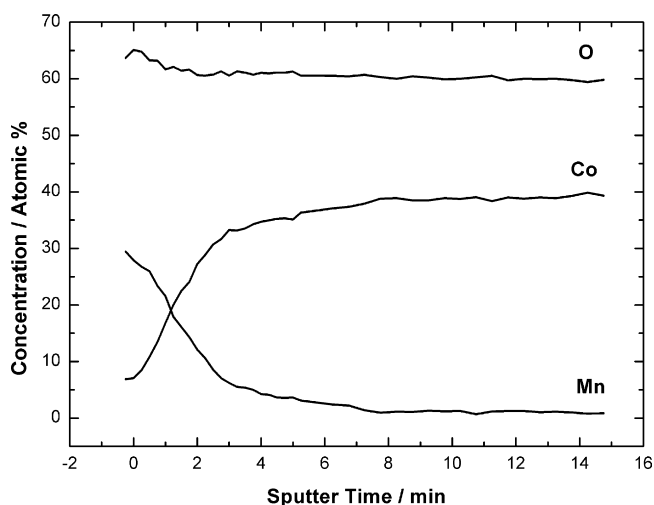


Fig. 4. Concentration profiles of LiMn_2O_4 -coated LiCoO_2 film by the AES analysis.

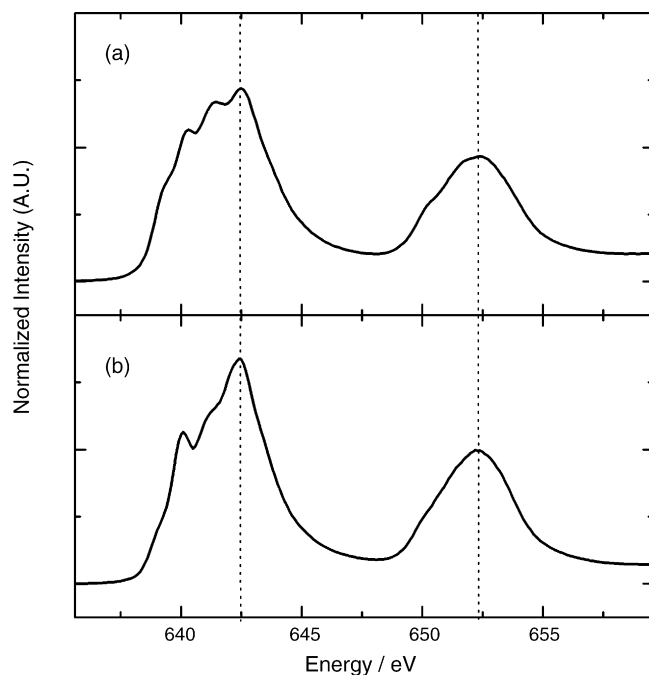


Fig. 5. Normalized Mn $L_{\text{II,III}}$ -edge X-ray absorption spectra of (a) LiMn_2O_4 and (b) LiMn_2O_4 -coated LiCoO_2 film.

transitions of Mn $2p_{3/2}$ and $2p_{1/2}$ core electrons, split by the spin-orbit interaction of the Mn $2p$ core level, to an unoccupied $3d$ level hybridized with oxygen $2p$ orbital, respectively. The Mn $L_{\text{II,III}}$ -edge XAS spectrum of LiMn_2O_4 -coated LiCoO_2 film is slightly different from that of LiMn_2O_4 . Based on the earlier soft XAS results of $\text{Li}_{1-x}\text{Mn}_2\text{O}_4$ during charge [18], it is clear that the oxidation state of Mn ions at the surface of LiMn_2O_4 -coated LiCoO_2 film is slightly higher than 3.5, which suggests that the structure at the surface of LiMn_2O_4 -coated LiCoO_2 film is a spinel $\text{LiCo}_x\text{Mn}_{2-x}\text{O}_4$. In order to make a clear comparison, we reproduce the Mn L -edge XAS spectra of $\text{Li}_{1-x}\text{Mn}_2\text{O}_4$ during charge in Fig. 6.

Fig. 7 shows normalized O K -edge X-ray absorption spectra of LiMn_2O_4 and LiMn_2O_4 -coated LiCoO_2 film. The spectrum of LiMn_2O_4 shows intense absorption peaks (A and B) at ~ 530 and ~ 532 eV and broad higher energy peaks (C and D) above 535 eV. The first intense pre-edge peaks (A and B) corresponds to the transition of oxygen $1s$ electron to the hybridized state of Mn $3d$ and oxygen $2p$ orbitals, whereas the broad higher energy peaks correspond to the transitions to hybridized states of oxygen $2p$ and Mn $4sp$ orbitals. Although the oxygen $1s \rightarrow$ Mn $3d$ transition is forbidden by the electric-dipole approximation, the appearance of the absorption peak is caused by the hybridization of Mn $3d$ and oxygen $2p$ orbitals. In this case, the first structure at 531 eV is assigned to a superposition of majority (spin-up) e_g and minority (spin-down) t_{2g} bands. On the other hand, the second structure at 533 eV is attributed to a band of minority e_g character. The peak features in the spectrum of LiMn_2O_4 -coated LiCoO_2 film is very similar to that of LiMn_2O_4 suggesting that the surface coating layer has spinel LiMn_2O_4 -based structure. It is observed that the pre-edge peaks (A and B) of LiMn_2O_4 -coated LiCoO_2 film slightly shifted to the higher energy, which

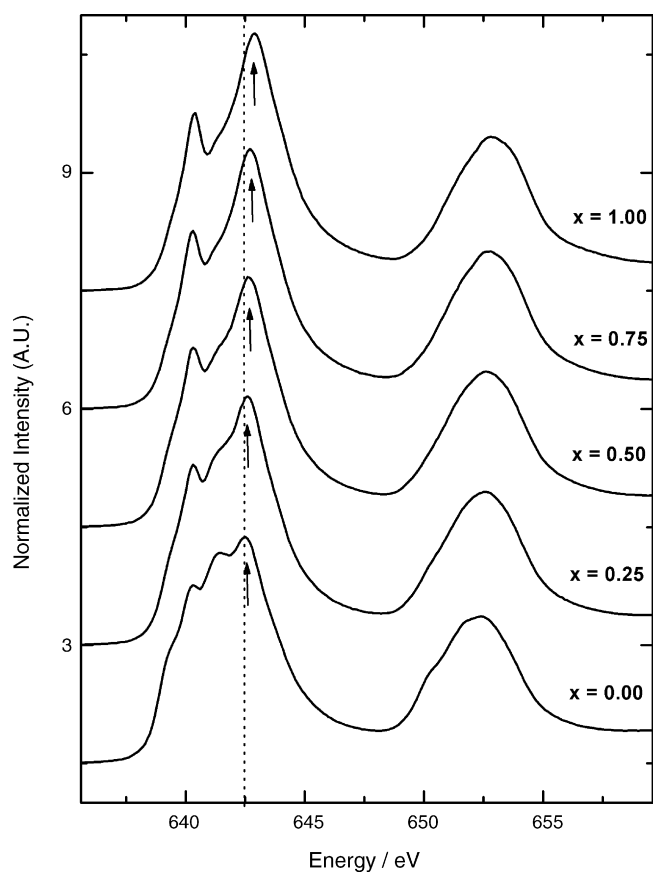


Fig. 6. Normalized Mn $L_{II,III}$ -edge X-ray absorption spectra of $Li_{1-x}Mn_2O_4$ system with respect to the x value.

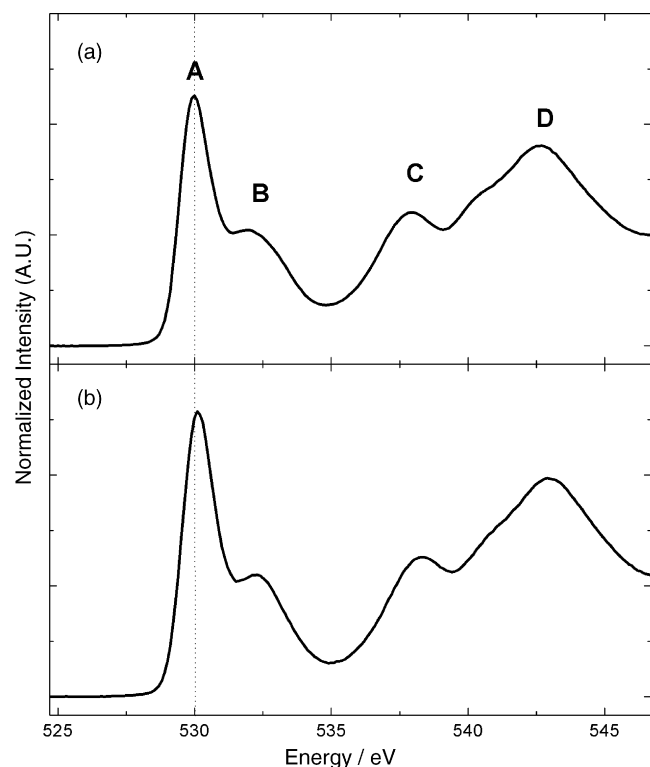


Fig. 7. Normalized O K-edge X-ray absorption spectra of (a) $LiMn_2O_4$ and (b) $LiMn_2O_4$ -coated $LiCoO_2$ film.

could be attributed to Co-doping effect in the spinel $LiMn_2O_4$ structure.

4. Conclusions

The $LiMn_2O_4$ -coated $LiCoO_2$ film electrode was successfully synthesized by ESD method. XRD and CV results showed that $LiMn_2O_4$ -coated $LiCoO_2$ film electrode is very similar to conventional $LiCoO_2$ film electrode in terms of bulk structure and electrochemical property. However, DSC results revealed that $LiMn_2O_4$ -coated $LiCoO_2$ film show better thermal stability than bare $LiCoO_2$ film. AES results showed that the Mn atoms are distributed only at the film surface region. From the observation of soft XAS spectra at the O K-edge and the Mn L-edge, it is concluded that the structure at the surface of $LiMn_2O_4$ -coated $LiCoO_2$ film is spinel $LiCo_xMn_{2-x}O_4$.

Acknowledgments

The work done at BNL was supported by the Assistant Secretary for Energy Efficiency and Renewable Energy, Office of FreedomCAR and Vehicle Technologies of the U.S. Department of Energy under Contract Number DE-AC02-98CH10886. The work done at Yonsei University was supported by the Korea Science and Engineering Foundation (KOSEF) through the Research Center for Energy Conversion and Storage (RCECS), (No. 2000-2-30100-012-3) and by the Ministry of Information and Communication of Korea [Support Project of University Information Technology Research Center, supervised by the Institute of Information Technology Assessment (IITA)].

References

- [1] K. Mizushima, P.C. Jones, P.C. Wiseman, J.B. Goodenough, *Mater. Res. Bull.* 15 (1980) 783.
- [2] T. Nagaura, K. Tozawa, *Prog. Batt. Solar Cells* 9 (1991) 209.
- [3] B. Wang, J.B. Bates, F.X. Hart, B.C. Sales, R.A. Zuhr, J.D. Robertson, *J. Electrochem. Soc.* 143 (1996) 3203.
- [4] C. Chen, E.M. Kelder, M.J.G. Jak, J. Schoonman, *Solid State Ionics* 86–88 (1996) 1301.
- [5] C. Chen, E.M. Kelder, P.J.J.M. van der Put, J. Schoonman, *J. Mater. Chem.* 6 (1996) 765.
- [6] J. Cho, G.B. Kim, H.S. Lim, C.S. Kim, S.-I. Yoo, *Electrochem. Solid State Lett.* 2 (1999) 607.
- [7] J. Cho, Y.J. Kim, T.J. Kim, B. Park, *Chem. Mater.* 13 (2001) 18.
- [8] Y.J. Kim, T.J. Kim, J.W. Shin, B. Park, J. Cho, *J. Electrochem. Soc.* 149 (2002) A1337.
- [9] A. Montoro, M. Abbate, J.M. Rosolen, *J. Electrochem. Soc.* 147 (2000) 1651.
- [10] Y. Uchimoto, H. Sawada, T. Yao, *J. Synchrotron. Rad.* 8 (2001) 872.
- [11] W.-S. Yoon, K.-B. Kim, M.-G. Kim, M.-K. Lee, H.-J. Shin, J.-M. Lee, J.-S. Lee, C.-H. Yo, *J. Phys. Chem. B* 106 (2002) 2526.
- [12] F.M.F. de Groot, *J. Electron Spectrosc. Relat. Phenom.* 67 (1994) 529.
- [13] W.-S. Yoon, S.-H. Ban, K.-K. Lee, K.-B. Kim, M.G. Kim, J.M. Lee, *J. Power Sources* 97–98 (2001) 282.
- [14] T.N. Lee, M.H. Yoon, Y.S. Kim, H.G. Kim, *Aust. J. Phys.* 48 (1995) 321.
- [15] H.J. Shin, Y. Chung, B. Kim, *J. Synchrotron. Rad.* 5 (1998) 648.
- [16] I. Uchida, H. Saito, *J. Electrochem. Soc.* 142 (1995) L139.
- [17] Z. Zhang, D. Fouchard, J.R. Rea, *J. Power Sources* 70 (1998) 16.
- [18] W.-S. Yoon, K.Y. Chung, K.-H. Oh, K.-B. Kim, *J. Power Sources* 119 (2003) 706.